

Unifying the phase diagrams of the magnetic and transport properties of $\text{La}_{2-x}\text{Sr}_x\text{CuO}_4$, $0 \leq x \leq 0.05$

E. Lai and R. J. Gooding

Department of Physics, Queen's University, Kingston, Ontario, Canada K7L 3N6

(Received 27 August 1997)

An extensive experimental and theoretical effort has led to a largely complete mapping of the magnetic phase diagram of $\text{La}_{2-x}\text{Sr}_x\text{CuO}_4$, and a microscopic model of the spin textures produced in the $x \leq 0.05$ regime has been shown to be in agreement with this phase diagram. Here we use this *same* model to derive a theory of the impurity-dominated, low-temperature transport. Then, we present an analysis of previously published data for two samples: $x=0.002$ data from Chen *et al.*, and $x=0.04$ data from Keimer *et al.* We show that the transport mechanisms in the two systems are the same, even though they are on opposite sides of the observed insulator-to-metal transition. Our model of impurity effects on the impurity-band conduction, variable-range-hopping conduction, and Coulomb-gap conduction is similar to that used to describe doped semiconductors. However, for $\text{La}_{2-x}\text{Sr}_x\text{CuO}_4$ we find that in addition to impurity-generated disorder effects, strong correlations are important and must be treated on an equal level with disorder. On the basis of this work we propose a phase diagram that is consistent with all available magnetic and transport experiments, and which connects the undoped parent compound with the lowest x value for which $\text{La}_{2-x}\text{Sr}_x\text{CuO}_4$ is found to be superconducting, viz. $x \approx 0.05$. [S0163-1829(98)10203-5]

I. INTRODUCTION

The transport properties of $\text{La}_{2-x}\text{Sr}_x\text{CuO}_4$ at low temperatures have attracted considerable attention recently, in particular, because it seems that for underdoped, superconducting Sr levels ($0.05 \leq x \leq 0.15$) the normal state (superconductivity suppressed by the application of a magnetic field) might be insulating.^{1,2} In this paper we present a theory for the transport properties of $\text{La}_{2-x}\text{Sr}_x\text{CuO}_4$ for $x \leq 0.05$ with the expectation that one can better understand the superconducting compounds if one first understands the weakly and moderately doped nonsuperconducting materials. Our theory relies on treating the effects of strong correlations and disorder with equal importance.

We employ a simple model to explain the low-temperature transport (resistivity and magnetoresistance) of $\text{La}_{2-x}\text{Sr}_x\text{CuO}_4$ for $0.0 \leq x \leq 0.05$, and examine the evolution that occurs as the system is doped from the antiferromagnetic insulator regime to the spin-glass phase. We stress that this model is not a new invention contrived just to explain this data. Instead, this same model has proven successful in describing quantitatively the magnetic "spin texture" of this system^{3,4} for $0.0 \leq x \leq 0.05$. If any model is indeed a physically realistic representation of $\text{La}_{2-x}\text{Sr}_x\text{CuO}_4$ it should be able to explain all of the physics of this material, not just the magnetic or transport properties. Thus, our present work on the application of this same model to the transport behavior in $\text{La}_{2-x}\text{Sr}_x\text{CuO}_4$ can be viewed as a critical test of the model. We find both qualitative and quantitative agreement between this model and published data.

II. MODELING OF THE TRANSPORT DATA

A. Approximations of our transport model

To begin, let us clearly spell out the approximations implicit in our transport model. Assuming that the Sr impurities

pin the carriers at low doping and low temperatures, it is now well established (see Refs. 5–7) that the ground state corresponds to carriers circulating either clockwise or counterclockwise around the impurity. Thus, one possible way to treat the coupling of the hole motion to the magnetic background is to realize that the presence of strong correlations changes the ground state from that of a circularly symmetric, *s*-wave impurity ground state, as is usually assumed, e.g., for doped semiconductors, to that of a doubly degenerate state with chiral quantum number $\omega = \pm i$;⁶ we refer to this as a chiral impurity ground state. As mentioned above, this model has been exploited in quantitatively explaining a variety of experiments^{8–10,3} concerning the magnetic properties of $\text{La}_{2-x}\text{Sr}_x\text{CuO}_4$. In order to make progress on the modeling of the transport data we proceed as follows.

A hole in the chiral impurity ground state circulates either clockwise or counterclockwise around a plaquette on the CuO_2 plane. For our transport analysis we determine a continuum approximation for the chiral impurity ground-state wave function by examining the Schrödinger equation in the effective-mass approximation. We assume that the hole is confined to the plane, so $\psi(x, y) = \psi(r, \phi)$. Then,

$$-\frac{\hbar^2}{2m^*} \nabla^2 \psi - \frac{e^2}{\epsilon_{\perp} \sqrt{r^2 + d_{\perp}^2}} \psi = E \psi, \quad (2.1)$$

where the potential follows from the location of the impurities above or below each CuO_2 plane, and the out-of-plane dielectric constant ϵ_{\perp} . For $\text{La}_{2-x}\text{Sr}_x\text{CuO}_4$ the appropriate numbers are $m^* \approx 1-2$ (we use 1.5), $d_{\perp} \approx 1.85$ Å, and $\epsilon_{\perp} \approx 31$.¹¹ (We note that experiment has shown¹² that ϵ_{\perp} is effectively independent of doping in the range $0 \leq x \leq 0.02$.) Mimicking the circulating character of the ground state we determine the wave functions of the form $\exp(\pm i\phi)$.

To compute the radial component of the wave function we note that for $\omega = \pm i$ states asymptotically far from the impurity the Schrödinger equation reduces to a form whose (radial) solutions can be expressed in terms of Kummer's function. Then, using the asymptotic properties of these functions, one finds that the continuum approximation to the impurity wave function are

$$\psi(r, \phi) \sim r e^{-r/a} e^{\pm i \phi} \quad (2.2)$$

where $a = (\epsilon_{\perp} \hbar^2 / 2m^* e^2)$. Using the numbers for $\text{La}_{2-x}\text{Sr}_x\text{CuO}_4$ given above, one has $a \approx 5.48 \text{ \AA}$. Of course, one may also solve the radial Schrödinger equation for this problem numerically, and in what follows all quantitative results are derived from this more precise determination of the impurity wave function.

From now on we assume that transport proceeds by holes moving between different impurity states, and ignore the effect of strong correlations on the interimpurity transit. That is, we include the effects of strong correlations only by their influence on the specification of the *symmetry* of the impurity ground states. If the hole motion is between distant sites (as in Mott variable-range hopping), or between neighboring impurity sites (as in thermally activated, impurity-band conduction), we simply use the numerical solution of Eq. (2.1) with chiral symmetry to predict the transport behavior of $\text{La}_{2-x}\text{Sr}_x\text{CuO}_4$.

B. Derivations of conductivity for different temperature regimes

Using the formalism of the Miller and Abrahams random resistor network model,¹³ one can compute the transition probability $\langle \gamma_{ij} \rangle$ between any two impurity sites i and j . In what follows we will present the resulting formulas for both the s -wave impurity ground states, such that the relation with traditional doped semiconductor work is clear, and for our chiral impurity ground states.

For s -wave symmetry impurity states, one finds

$$\langle \gamma_{ij}^s \rangle \sim r_{ij}^{2d-4} \exp\left(-\frac{2r_{ij}}{a} - \frac{\epsilon_{ij}}{k_B T}\right), \quad (2.3)$$

where $d=2,3$ is the dimensionality, r_{ij} is the distance between the two sites, and ϵ_{ij} is the difference in on-site energies between the two sites. The activated form is well known, but the prefactor may not be; in fact, usually the prefactor is ignored. However, this dependence has appeared in the literature previously [see, e.g., Ref. 13, Eqs. (4.2.17,18)].

The corresponding result for the chiral impurity ground states is

$$\langle \gamma_{ij}^x \rangle \sim r_{ij}^{2d} \exp\left(-\frac{2r_{ij}}{a} - \frac{\epsilon_{ij}}{k_B T}\right). \quad (2.4)$$

Note that the only change is in the r dependence of the prefactor.

Applying percolation theory¹³ to Eqs. (2.3,2.4), one may derive the conductivity for these theories as a function of temperature, and three different regimes are found. The transport is always phonon assisted in that energy must be supplied to (absorbed from) a hole localized on site i in order

that it can move to site j (assuming that site j is unoccupied). At high temperatures, there are phonons of all energies available, so that the hole can always hop to its neighboring impurity site, regardless of the difference in their on-site energies. Hence, nearest-neighbor, or so-called impurity band conduction (IBC), takes place. The conductivity is then given by

$$\sigma_{\text{IBC}}(T) \sim \exp\left(-\frac{\epsilon_c}{k_B T}\right), \quad (2.5)$$

where ϵ_c is the average activation energy needed for a carrier to move to its neighboring site. This result is independent of dimensionality and the symmetry of the impurity ground state.

As the temperature is lowered, motion between neighboring sites may be forbidden due to the lack of phonons of appropriate energy. Consequently, it is more likely for the carriers to hop to a more distant site if this means that the energy difference is less. This is known as Mott variable range hopping (VRH). The conductivity for d -dimensional variable range hopping for conventional s -wave impurities is given by the familiar expression

$$\sigma_{\text{VRH},s}(T) \sim \left(\frac{1}{T}\right)^{(2d-4/d+1)} \exp\left[-\left(\frac{T_d}{T}\right)^{1/(d+1)}\right], \quad (2.6)$$

where T_d is a characteristic temperature given by

$$T_3 = \frac{22.8}{g(\mu) k_B a^3}, \quad (2.7)$$

$$T_2 = \frac{13.8}{g(\mu) k_B a^2} \quad (2.8)$$

for three and two dimensions, respectively. Here $g(\mu)$ is the density of states at the Fermi level, which is assumed to be constant in the VRH regime.¹³ Ignoring the prefactor, as is usually done,¹³ for 3D systems one has the familiar ‘‘Mott 1/4 law’’ for VRH. For the chiral impurity ground states that we are considering, one finds

$$\sigma_{\text{VRH},x}(T) \sim \left(\frac{1}{T}\right)^{(2d/d+1)} \exp\left[-\left(\frac{T_d}{T}\right)^{1/(d+1)}\right], \quad (2.9)$$

and thus only the temperature dependence of the prefactor is different.

For temperatures so low that the energy difference between the initial and final site is comparable to the Coulomb correlation energy between carriers, the density of states near the Fermi level is no longer constant. Instead, Coulomb interactions cause the density of states to vanish at the Fermi level,¹³ and a Coulomb gap is formed. A model known as the Coulomb gap (CG) model can be used to describe the conductivity in this situation, and the result is

$$\sigma_{\text{CG},s}(T) \sim \left(\frac{1}{T}\right)^{d-2} \exp\left[-\left(\frac{T_{\text{ES}}}{T}\right)^{1/2}\right] \quad (2.10)$$

for s -wave states, where

TABLE I. Summary of the differing temperature dependencies of the conductivity.

IBC	$\sigma_{\text{IBC}}(T) \propto \exp(-\epsilon_c/k_B T)$
3D <i>s</i> -wave VRH	$\sigma_{\text{VRH},s}(T) \propto T^{-2/3} \exp[-(T_3/T)^{1/4}]$
2D <i>s</i> -wave VRH	$\sigma_{\text{VRH},s}(T) \propto \exp[-(T_2/T)^{1/3}]$
3D chiral VRH	$\sigma_{\text{VRH},\chi}(T) \propto T^{-3/2} \exp[-(T_3/T)^{1/4}]$
2D chiral VRH	$\sigma_{\text{VRH},\chi}(T) \propto T^{-4/3} \exp[-(T_2/T)^{1/3}]$
3D <i>s</i> -wave CG	$\sigma_{\text{CG},s}(T) \propto T^{-1} \exp[-(T_{\text{ES}}/T)^{1/2}]$
2D <i>s</i> -wave CG	$\sigma_{\text{CG},s}(T) \propto \exp[-(T_{\text{ES}}/T)^{1/2}]$
3D chiral CG	$\sigma_{\text{CG},\chi}(T) \propto T^{-3} \exp[-(T_{\text{ES}}/T)^{1/2}]$
2D chiral CG	$\sigma_{\text{CG},\chi}(T) \propto T^{-2} \exp[-(T_{\text{ES}}/T)^{1/2}]$

$$T_{\text{ES}} = \frac{2.9e^2}{\epsilon_{\parallel} a k_B}, \quad (2.11)$$

where ES denotes the theory of Efros and Shklovskii and ϵ_{\parallel} is the in-plane dielectric constant. The corresponding result for chiral impurity states is

$$\sigma_{\text{CG},\chi}(T) \sim \left(\frac{1}{T}\right)^d \exp\left[-\left(\frac{T_{\text{ES}}}{T}\right)^{1/2}\right]. \quad (2.12)$$

The exponent 1/2 inside the exponential factor is the same for both two and three dimensions, but again the prefactors depend on the symmetry of the impurity ground state.

This sequence of impurity-dominated transport as a function of temperature, viz. IBC at high temperatures, VRH at intermediate temperatures, followed by CG transport at low temperatures, has been observed in a number of experimental systems. For example, in amorphous Ge IBC has been observed for $T \gtrsim 200$ K, VRH conduction occurs for $2 \text{ K} \lesssim T \lesssim 200 \text{ K}$,¹⁴⁻¹⁶ and CG conduction was observed for $T \lesssim 2 \text{ K}$.¹⁴⁻¹⁶ However, the prefactors that we have obtained were not included in these analyses. In what follows we use these terms to determine the impurity ground-state symmetry, and find strong support for the chiral impurity ground-state model used previously to describe successfully the magnetic properties of $\text{La}_{2-x}\text{Sr}_x\text{CuO}_4$.

C. Analysis of previously published conductivity data

In the previous section we presented our predictions for the temperature dependence of the conductivity due to various kinds of hopping conduction processes in different temperature regimes. The expressions for these conductivities are summarized in Table I. In order to fit these expressions to data, we note that for all theories there are two fitting parameters. Thus, minimizing the χ^2 of a fit is equivalent to maximizing the goodness of fit parameter, and in what follows we only refer to χ^2 .

TABLE III. Comparison of the IBC and the weak localization predictions for the $x=0.04$ Keimer data, for $20 \text{ K} \leq T \leq 70 \text{ K}$.

	IBC	Weak localization
χ^2	0.000618	0.0142

The first data that we analyzed were those of a $x=0.002$ single crystal prepared by Chen *et al.*¹¹ Their analysis ignored the temperature prefactors mentioned above, and led to the conclusion that the transport in this weakly doped anti-ferromagnet could be described by conventional doped semiconductor theory. In particular, IBC was observed for $50 \text{ K} \lesssim T \lesssim 295 \text{ K}$, while for $4 \text{ K} \lesssim T \lesssim 50 \text{ K}$ they found that the conduction mechanism is that of the traditional 3D Mott VRH type. No data below 4 K were taken, and thus no evidence of CG conduction was found.

We agree with their interpretation of IBC for $50 \text{ K} \lesssim T \lesssim 295 \text{ K}$, and from our fit we find $\epsilon_c \approx 0.020 \text{ eV}$ as the average activation energy needed for the hop. However, for $4 \text{ K} \lesssim T \lesssim 50 \text{ K}$, we find that the chiral VRH expression from Eq. (2.9) with $d=2$ gives a better fit to the conductivity data. A comparison of all four VRH hopping theories mentioned above is provided in Table II.

We also studied the conductivity data of an $x=0.04$ single crystal prepared by Keimer *et al.*⁹ For reasons that are unclear to us, around 50 K only one conductivity theory was compared to the data, that being appropriate for a system displaying 2D weak localization. For such a system one predicts a logarithmic dependence of temperatures (which also has two fitting parameters). These authors suggested that such a conduction mechanism was operative from $10 \text{ K} \lesssim T \lesssim 100 \text{ K}$. Then, for $1 \text{ K} \lesssim T \lesssim 10 \text{ K}$ the system was in a ‘‘crossover’’ regime, and then for $T \lesssim 1 \text{ K}$ the system displayed CG conduction. Clearly, if such a description were true, except at the lowest temperatures the conduction mechanisms of the $x=0.002$ and the $x=0.04$ systems would have nothing to do with one another.

In contrast to this approach, we disagree with using weak-localization theory to account for the conduction mechanism in $\text{La}_{2-x}\text{Sr}_x\text{CuO}_4$ around 50 K. Firstly and most importantly, weak localization theory fails to include the strong correlation effects between the hole and the background Cu spins, in direct contrast to what is made manifest by studies of the magnetic properties of this material. Secondly, such behavior is completely at odds with the negative, *isotropic* magnetoresistance observed by this same group.¹⁷ After reanalyzing their conductivity data, we find a much simpler and more natural explanation—for $20 \text{ K} \lesssim T \lesssim 70 \text{ K}$, Eq. (2.5), the simple activated expression for IBC, gives a much better fit than the logarithmic temperature dependence arising from weak-localization theory. The χ^2 for these fits is listed in Table III, and it is seen that IBC has a χ^2 at least 20 times less than the corresponding χ^2 for logarithmic temperature

TABLE II. Comparison of VRH theories for the $x=0.002$ Chen data, for $50 \text{ K} \leq T \leq 295 \text{ K}$.

	3D <i>s</i> -wave VRH	2D <i>s</i> -wave VRH	3D chiral VRH	2D chiral VRH
χ^2	0.411	0.371	0.317	0.169
T_d	$5.1 \times 10^6 \text{ K}$	$6.7 \times 10^4 \text{ K}$	$9.3 \times 10^6 \text{ K}$	$1.3 \times 10^5 \text{ K}$

TABLE IV. Comparison of VRH theories for the $x=0.04$ Keimer data, for $1\text{ K} \leq T \leq 20\text{ K}$.

	3D s -wave VRH	2D s -wave VRH	3D chiral VRH	2D chiral VRH
χ^2	0.0756	0.0795	0.0823	0.0483
T_d	$2.7 \times 10^4\text{ K}$	550 K	$1.2 \times 10^5\text{ K}$	630 K

dependence. The average activation energy found from the fit is $\epsilon_c \approx 0.002\text{ eV}$, roughly a factor of 10 less than that for the $x=0.002$ sample. The poor comparison of weak-localization theory is not improved when a different temperature regime is used.

If our chiral impurity model is indeed correct, and weak localization is not found for this system, it should exhibit a crossover from IBC to VRH as the temperature is lowered, and this is precisely what we find. For $1\text{ K} \leq T \leq 20\text{ K}$, we find that Eq. (2.9) with $d=2$, the expression for 2D chiral VRH again gives the best fit to the conductivity data—the statistical data are listed in Table IV.

Below 1 K we find that Eq. (2.12) with $d=2$, the expression for 2D chiral impurity Coulomb gap hopping gives the best fit to the conductivity data; Table V summarizes the statistical data.

In *all* cases discussed above, the best fit to the data is found to correspond to our 2D chiral impurity ground-state theory. We believe that this *repeated agreement* between theory and experiment lends strong credibility to our model, an argument that is further strengthened when it is noted that this same model successfully describes the magnetic properties of $\text{La}_{2-x}\text{Sr}_x\text{CuO}_4$.

D. Crossover temperatures

In the previous section we showed that our 2D chiral conduction model, which follows from the chiral impurity ground state generated by strong correlations, fits the experimental data better than other available theories. Further quantitative support for this theory follows from a study of the crossover temperatures, which we now present.

For the $x=0.002$ crystal there is a crossover from IBC to 2D chiral VRH conduction at around 50 K. For the $x=0.04$ crystal, the crossover from IBC to 2D chiral VRH conduction occurs at around 20 K. Then, the crossover to 2D chiral CG conduction occurs at around 1 K.

One may determine these crossover temperatures semiempirically. That is, in what follows we derive the crossover temperatures theoretically, but our formulas involve parameters that we cannot determine. However, we can express these parameters in terms of the activation energy ϵ_c , and the characteristic temperatures T_2 and T_{ES} . All of these numbers were determined in the previous section from the fits of our model to the experimental data, and are stated in the text and/or listed in the Tables.

TABLE V. Comparison of CG theories for the $x=0.04$ Keimer data, for $T < 1\text{ K}$.

	3D s -wave CG	2D s -wave CG	3D chiral CG	2D chiral CG
χ^2	0.291	0.286	1.633	0.271
T_{ES}	30 K	51 K	80 K	32 K

The crossover between IBC and VRH can be estimated from the condition that the average activation energy between neighboring sites is equal to the activation energy for carriers executing variable range hopping. The latter quantity can be determined from expressing the hopping distance between two sites in terms of the activation energy, and then setting the hopping distance to be the average distance as a function of temperature. That is, the activation energy for carriers executing variable range hopping is given by $-d\ln\sigma_{\text{VRH}}/d\beta$,¹⁵ where $\beta \equiv 1/k_B T$, and σ_{VRH} is given by the chiral expression in Eq. (2.9) with $d=2$. Hence, by solving

$$\epsilon_c = -\frac{d\ln(\sigma_{\text{VRH}})}{d\beta}, \quad (2.13)$$

one obtains

$$T_{\text{IBC} \rightarrow \text{VRH}} = \frac{1}{\sqrt{T_2}} \left(\frac{3\epsilon_c}{k_B} \right)^{3/2}. \quad (2.14)$$

For the $x=0.002$ crystal, we take $T_2 = 1.3 \times 10^5\text{ K}$ from Table II, and our fit to IBC yielded $\epsilon_c = 0.020\text{ eV}$. This produces $T_{\text{IBC} \rightarrow \text{VRH}} = 51\text{ K}$, in good agreement with the experimental value of 50 K.¹¹ For the $x=0.04$ crystal we take $T_2 = 630\text{ K}$ from Table IV, and our fit yielded $\epsilon_c = 0.002\text{ eV}$. This gives $T_{\text{IBC} \rightarrow \text{VRH}} = 23\text{ K}$, again in good agreement with the experimental value of 20 K.⁹

One may derive the crossover temperature from VRH to CG conduction as well. As discussed previously, this crossover occurs when the Coulomb correlation energy between carriers is equal to the activation energy needed to hop to a distant site. The former is given by $e^2/\epsilon_{\parallel} \bar{r}$, where \bar{r} is the most likely hopping distance for variable range hopping. Hence by solving

$$e^2/\epsilon_{\parallel} \bar{r} = -\frac{d\ln(\sigma_{\text{VRH}})}{d\beta} \quad (2.15)$$

one obtains

$$T_{\text{VRH} \rightarrow \text{CG}} = 33.2 \frac{T_{\text{ES}}^3}{T_2^2} \quad (2.16)$$

as the crossover temperature between variable range hopping and Coulomb gap conduction.

For the $x=0.04$ crystal, $T_2 = 630\text{ K}$ from Table IV and $T_{\text{ES}} = 32\text{ K}$ from Table V. This gives $T_{\text{VRH} \rightarrow \text{CG}} \approx 2\text{ K}$, again in good agreement with the experimental value of 1 K.⁹

The other theories discussed in the previous sections can also be used to calculate crossover temperatures, but none of these sets of temperatures accurately tracks the experimental crossover temperatures as well as our 2D chiral theory. Thus, this set of crossover temperatures provides further support quantitatively for our model.

III. METAL-TO-NONMETAL TRANSITION DOPING CONCENTRATION

$\text{La}_{2-x}\text{Sr}_x\text{CuO}_4$ is a strongly correlated electronic system that is greatly influenced by the disorder effects produced by the Sr impurities. This view is made clear by the above transport work and previously published work on the magnetic properties.³ It is known that this system undergoes a nonmetal-to-metal transition with increasing doping level x , and in this section we employ our chiral impurity model to show that it also reproduces the experimental value for the critical doping level, $x_c \approx 0.02$. However, before proceeding to this derivation, we wish to present a clear discussion of how we believe this transition should be viewed, since confusing and conflicting remarks dominate the literature on this subject.

The conventional view of a nonmetal-to-metal transition in a disordered system has been demonstrated for many experimental systems; here we use the recent, elegant work of Dubon *et al.*,¹⁸ for Ge (under stress) doped with Cu impurities to demonstrate this. Upper and lower Hubbard impurity ‘‘bands’’ form, and the gap separating these bands decreases with increasing impurity concentration. The critical concentration is that at which this gap closes. However, for Cu doping levels beyond the critical concentration, the transport at low temperatures is still found to be insulatinglike, viz. the resistivity increases with decreasing temperature¹⁹—only at higher temperatures is the chemical potential pushed through the mobility edge and metallic conduction found. This phenomenology thus implies that the temperature at which metallic conduction is found (by which we imply that the resistivity increases with increasing temperature) is concentration dependent, and that the critical concentration for the nonmetal-to-metal transition is the doping level for which metallic conduction is first found at high temperatures.

This picture is consistent with published transport data for $\text{La}_{2-x}\text{Sr}_x\text{CuO}_4$ at low and intermediate doping levels: At the lowest Sr levels the resistivity is always found to be insulatinglike,^{11,20} while for larger x (Ref. 21) only at high temperatures does the resistivity increase (approximately linearly) with increasing temperature. This is further substantiated from the dielectric constant measurements of Chen *et al.*¹² who found that the in-plane dielectric constant of $\text{La}_{2-x}\text{Sr}_x\text{CuO}_4$ saturated at high frequencies, and this saturation value diverged at some doping level. It is difficult to infer the critical x value from this experiment, and in what follows we use $x_c \approx 0.02 \pm 0.005$ as a reasonable approximation for the critical concentration of the metal-to-nonmetal transition.

Our chiral impurity model can be used to estimate the critical doping concentration for $\text{La}_{2-x}\text{Sr}_x\text{CuO}_4$ via the Mott-Hubbard treatment of such transitions. The overlap integral between impurity sites separated by a distance r , and the on-site Coulomb repulsion for two holes being at one impurity site, can be estimated using the wave function given in Eq. (2.2). Then, the Mott criterion corresponds to the doping level at which an impurity ‘‘band’’ has a width equal to the on-site Coulomb repulsion energy. These simple calculations²² lead to the 2D analogue of Mott’s criterion for chiral impurity ground states, viz.

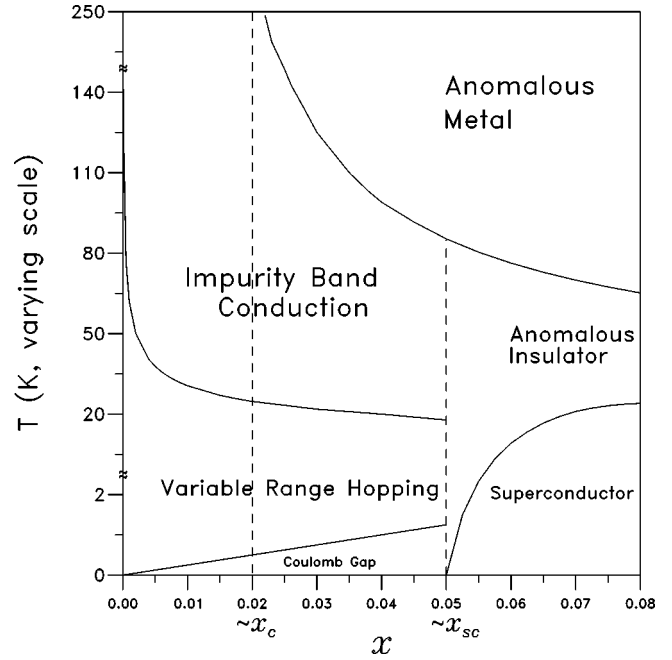


FIG. 1. $\rho_{ab}(T)$ phase diagram for $\text{La}_{2-x}\text{Sr}_x\text{CuO}_4$ summarizing its transport properties as inferred from our analysis. The dashed line at $x_c \approx 0.02$ is the critical doping concentration for the metal-to-nonmetal transition. The dashed line at $x_{sc} \approx 0.05$ is the onset for superconductivity—this vertical line on our phase diagram is a guide for the eye only. The anomalous metallic phase at high temperatures for $x > 0.02$ and the superconducting phase for $x > 0.05$ are also shown in this figure. The nature and the extent of the ‘‘anomalous insulator’’ part of the phase diagram is not yet known.

$$x_c^{1/2} \left(\frac{a}{a_0} \right) \approx 0.191, \quad (3.1)$$

where a is the effective Bohr radius of the chiral impurity ground state (stated previously to be 5.48 \AA), and $a_0 = 3.85 \text{ \AA}$ is the planar lattice constant. Solving this equation we find $x_c \approx 0.018$, in good agreement with experiment. The fact that our theory is *two* dimensional agrees also with the experimental fact that even though the in-plane dielectric constant at high frequencies diverges at x_c , the out-of-plane dielectric constant remains roughly constant as x_c is approached.¹² Thus, quantitatively and qualitatively, we find that our chiral impurity model is consistent with available, published transport data on the metal-to-nonmetal transition.

IV. ρ_{ab} PHASE DIAGRAM

Figure 1 shows the approximate ρ_{ab} transport phase diagram for the new hopping conduction mechanism that we propose for $x \leq 0.05$, and summarizes our results. From this figure it is clear that our work supports the contention that at low temperatures the conduction mechanism on either side of the metal-to-nonmetal transition ($x_c \approx 0.02$) is the same. This is in disagreement with the idea proposed in Ref. 9 that weak-localization effects are seen in the $x = 0.04$ transport data. For $x \geq 0.02$ and at high T , $\text{La}_{2-x}\text{Sr}_x\text{CuO}_4$ behaves like an anomalous metal with an approximate T -linear resistivity. Our theory has nothing to say about the dominant scattering mechanism that produces this unusual behavior.

In Fig. 1 the superconducting phase for $x \geq 0.05$ and $T < T_c$ is shown. The region between the superconducting phase and the anomalous metallic phase is referred to as an “anomalous insulator” phase according to Ando *et al.*¹ They examined the normal state properties of $\text{La}_{2-x}\text{Sr}_x\text{CuO}_4$ ($x = 0.08$ and $x = 0.013$) down to $T/T_c \approx 0.04$ by suppressing superconductivity with a pulsed magnetic field of 61 T along the c axis. They measured the in-plane resistivity ρ_{ab} and the out-of-plane resistivity ρ_c , and found insulating behavior for both resistivities at low temperatures. Under the assumption that the magnetic-field dependence of the resistivity is very small compared to the temperature dependence, Ando *et al.* claim that their materials are indeed insulating in the region labeled “anomalous insulator” in Fig. 1. [However, their main assumption has been challenged by the work of Malinowski *et al.*,² who claimed that the behavior observed in strong magnetic fields is not a reliable guide to the nature of the zero-field ground state in the absence of superconductivity. Malinowski *et al.* measured the normal-state conductances per CuO_2 plane for two highly underdoped superconducting $\text{La}_{2-x}\text{Sr}_x\text{CuO}_4$ samples ($x = 0.048$ and $x = 0.051$) at different fields, and their data are found to collapse onto one curve with the use of a single scaling parameter that is inversely proportional to the Bohr radius of the ground-state wave function. When extrapolated to zero field, this scaling parameter approaches zero, which suggests that the zero-field ground state may be extended, as opposed to localized (as suggested by Ando *et al.*). This discrepancy between the two groups has not yet been settled.]

The relationship of our work to this portion of the phase diagram is unclear. If disorder effects are important, then it is certainly possible that the anomalous insulating behavior (if truly present) might be related to the physics discussed in this paper. Alternatively, as proposed in Ref. 2, if the anomalous insulating behavior is associated with the magnetic field changing the electronic structure and subsequently producing localized states, then it is unlikely that our theory can be extrapolated to such doping levels.

Further, we hope that new data on traveling-solvent float-zone grown single crystals for a variety of doping levels

above and below $x = 0.05$ (Ref. 23) will allow for us to judge conclusively if it is appropriate to extrapolate our theory to the doping concentrations containing the superconducting samples.

V. SUMMARY

To summarize, we have presented a theory of the transport of $\text{La}_{2-x}\text{Sr}_x\text{CuO}_4$ for $x \leq 0.05$. It is to be emphasized that the physics that led to our theory, the chiral impurity ground state and the successful description of the spin texture of $\text{La}_{2-x}\text{Sr}_x\text{CuO}_4$ at low temperatures,³ are the same. Disorder and strong correlations dominate the low temperature, low doping regime of $\text{La}_{2-x}\text{Sr}_x\text{CuO}_4$.

One potential weakness of our work is that almost all of our comparisons are of a quantitative nature. Instead, one would like to compare the qualitative behavior found in certain transport measurements. To this end, we are presently preparing a manuscript on a comparison of our theory to the magnetoresistance measurements for samples in this same doping regime. In particular, such work allows for the scaling properties of a theory, with respect to field and temperature, to be compared to experiment. This theory is outside of the simple treatment of impurity-dominated hopping-type conduction given here, and will be reported elsewhere.

ACKNOWLEDGMENTS

We wish especially to thank Chih-Yung Chen and Bernhard Keimer for providing us with listings of their previously published data, and Shiki Ueki, Kazu Yamada, Yasuo Endoh, Lance Miller, and Oscar Dubon, for providing us with data prior to publication. One of us (R.J.G.) wishes to thank Marc Kastner for introducing him to the MIT experimental work on this subject. We thank Lance Miller, Tom Timusk, Bob Birgeneau, and David Johnston for critical comments. This work was begun while one of us (R.J.G.) was visiting MIT and McMaster University, and he wishes to thank them for their hospitality. This work was supported by the NSERC of Canada.

¹Y. Ando, G. S. Boebinger, A. Passner, Tsuyoshi Kimura, and Kohji Kishio, *Phys. Rev. Lett.* **75**, 4662 (1995); Y. Ando, G. S. Boebinger, A. Passner, N. L. Wang, C. Geibel, and F. Steglich, *ibid.* **77**, 2065 (1996); G. S. Boebinger, Y. Ando, A. Passner, T. Kimura, M. Okuya, J. Shimoyama, K. Kishio, K. Tamasaku, N. Ichikawa, and S. Uchida, *ibid.* **77**, 5417 (1996); Y. Ando, G. S. Boebinger, A. Passner, Tsuyoshi Kimura, and Kohji Kishio, *J. Low Temp. Phys.* **105**, 867 (1996).

²K. Karpinska, A. Malinowski, M. Z. Cieplak, S. Guha, S. Gershman, G. Kotliar, T. Skoskiewicz, W. Plesiewicz, M. Berkowski, and P. Lindenfild, *Phys. Rev. Lett.* **77**, 3033 (1996); A. Malinowski, M. Z. Cieplak, A. S. van Steenberg, J. A. A. J. Perenboom, K. Karpinska, M. Berkowski, S. Guha, and P. Lindenfild, *ibid.* **79**, 495 (1997).

³R. J. Gooding, N. M. Salem, R. J. Birgeneau, and F. C. Chou, *Phys. Rev. B* **55**, 6360 (1997).

⁴R. J. Gooding, N. M. Salem, and A. Mailhot, *Phys. Rev. B* **49**, 6067 (1994).

⁵K. J. von Szczepanski, T. M. Rice, and F. C. Zhang, *Europhys. Lett.* **8**, 797 (1989).

⁶R. J. Gooding, *Phys. Rev. Lett.* **66**, 2266 (1991).

⁷K. M. Rabe and R. Bhatt, *J. Appl. Phys.* **69**, 4508 (1991).

⁸F. C. Chou, F. Borsa, J. H. Cho, D. C. Johnston, A. Lascialfari, D. R. Torgeson, and J. Ziolo, *Phys. Rev. Lett.* **71**, 2323 (1993).

⁹B. Keimer, N. Belk, R. J. Birgeneau, A. Cassanho, C. Y. Chen, M. Greven, M. A. Kastner, A. Aharony, Y. Endoh, R. W. Erwin, and G. Shirane, *Phys. Rev. B* **46**, 14 034 (1992).

¹⁰F. C. Chou, N. R. Belk, M. A. Kastner, R. J. Birgeneau, and A. Aharony, *Phys. Rev. Lett.* **75**, 2204 (1995).

¹¹C. Y. Chen, E. C. Branlund, ChinSung Bae, K. Yang, M. A. Kastner, A. Cassanho, and R. J. Birgeneau, *Phys. Rev. B* **51**, 3671 (1995).

- ¹²C. Y. Chen, N. W. Preyer, P. J. Picone, M. A. Kastner, H. P. Jenssen, D. R. Gabbe, A. Cassanho, and R. J. Birgeneau, *Phys. Rev. Lett.* **63**, 2307 (1989); N. W. Preyer, R. J. Birgeneau, C. Y. Chen, D. R. Gabbe, H. P. Jenssen, M. A. Kastner, P. J. Picone, and Tineke Thio, *Phys. Rev. B* **39**, 11 563 (1989); C. Y. Chen, R. J. Birgeneau, M. A. Kastner, N. W. Preyer, and Tineke Thio, *ibid.* **43**, 392 (1991).
- ¹³For a review, see B. I. Shklovskii and A. L. Efros, *Electronic Properties of Doped Semiconductors* (Springer-Verlag, New York, 1984).
- ¹⁴N. F. Mott, *Philos. Mag.* **26**, 1015 (1972).
- ¹⁵A. H. Clark, *Phys. Rev.* **154**, 750 (1967).
- ¹⁶G. Sadasiv, *Phys. Rev.* **128**, 1131 (1962).
- ¹⁷N. W. Preyer, M. A. Kastner, C. Y. Chen, R. J. Birgeneau, and Y. Hidaka, *Phys. Rev. B* **44**, 407 (1991).
- ¹⁸O. D. Dubon, W. Walukiewicz, J. W. Beeman, and E. E. Haller, *Phys. Rev. Lett.* **78**, 3519 (1997).
- ¹⁹O. Dubon (private communication).
- ²⁰One resistivity measurement of single crystal $\text{La}_{1.99}\text{Sr}_{0.01}\text{CuO}_4$ has been taken up to room temperature: A. Lacerda, T. Graf, J. H. Cho, J. D. Thompson, and M. P. Maley, *Physica C* **235-240**, 1353 (1994). L. Miller (private communication) has measured the in-plane resistivity of the related single-plane system $\text{Sr}_2\text{CuO}_2\text{Cl}_2$, which has an approximate doping level (in terms of the x variable describing the Sr levels of $\text{La}_{2-x}\text{Sr}_x\text{CuO}_4$) of $x \approx 0.009$. His data are consistent with the activated form of nearest-neighbor impurity band conduction, and was found to occur for $200 \text{ K} \leq T \leq 350 \text{ K}$. Around 375 K, the sample reduced in a reduced-oxygen atmosphere, and hence created problems for accurate measurements at higher temperatures.
- ²¹H. Takagi, B. Batlogg, H. L. Kao, J. Kwo, R. J. Cava, J. J. Krajewski, and W. F. Peck, *Phys. Rev. Lett.* **69**, 2975 (1992).
- ²²Implicit in this expression is the assumption that the effective coordination number is equal to 2, the dimensionality of the hopping conduction. This may be justified in general, as will be discussed in a future publication, or on the basis of the topology of the spin texture discussed in Ref. 1.
- ²³S. Ueki, K. Yamada, and Y. Endoh (private communication).